Characterizing Angular Dependence of Spin-Orbit Torque Effective Fields in Pt/(Co/Ni)$_2$/Co/IrMn Structure

Christian Engel, Sarjoosing Goolaup, Feilong Luo, and Wen Siang Lew

School of Physical and Mathematical Sciences, Nanyang Technological University, Singapore 637371

We investigate the interplay between the spin-orbit torque (SOT)-induced effective fields and the azimuth angle of the magnetization vector with respect to the applied current. A method to quantify the ratio of the planar Hall effect to the anomalous Hall effect in perpendicular magnetic anisotropy (PMA) structures by using the low field harmonic Hall voltage measurement technique is devised. The validity of the ratio is confirmed by measuring the PMA effective field. In addition, a technique to characterize the SOT effective fields as a function of the magnetization vector azimuth angle with respect to the current direction is proposed and experimentally validated. The experimental results are in quantitative agreement with our derivations. Our measurement reveals that the field-like effective SOT fields are minima when the azimuth angle of magnetization with respect to the current is at 45°.

Index Terms—**Magnetization angle dependence, spin-orbit torque (SOT).**

I. Introduction

SPIN-ORBIT torque (SOT) has drawn much attention as an efficient way to switch magnetization state via current [1]–[4], which is of great interest for spintronics devices such as magnetic random access memory. The structure exploiting spin-orbit coupling usually comprises of heavy metal (HM), ferromagnetic (FM), oxide trilayer where spin-polarized current arises due to spin Hall effect in the HM and Rashba effect at the interfaces. The coupling between spins of conduction electrons in HM and localized electrons in FM material influences the magnetization of the FM layer via the SOT. The intensity of the SOT is generally characterized by two effective fields: damping-like and field-like. These SOT effective fields are aligned longitudinal ($H_{\text{SOT-}X}$) or transverse ($H_{\text{SOT-}Y}$) to the current direction.

A quantitative method to characterizing the SOT effective fields has been derived using the harmonic Hall voltage measurement technique [7], [8]. For structures with perpendicular magnetic anisotropy (PMA), the measured Hall voltage generally comprises of the contribution from the anomalous Hall effect (AHE). However, the planar Hall effect (PHE) has been shown to influence the second harmonic Hall voltage and plays an unexpected role in determining the SOT effective fields [9], [10]. The complex interplay of SOT effective fields while rotating the magnetization vector with respect to the current direction has been investigated using the symmetry aspects of the angle between magnetization and current [4].

In this paper, we look at the interplay between the SOT-induced effective fields in systems with antiferromagnetic material and the angle which the magnetization vector makes with respect to the applied current. The SOT and magnetic anisotropy effective fields are studied in a Ta/Pt/(Co/Ni)$_2$/Co/IrMn/Ta material structure. A method to characterize the PHE at low external fields is proposed. The alternating current I_{ac} harmonic Hall measurement method is extended to enable angular dependence characterization of the SOT effective fields. A good agreement between our theoretical derivation and experimental result is obtained.

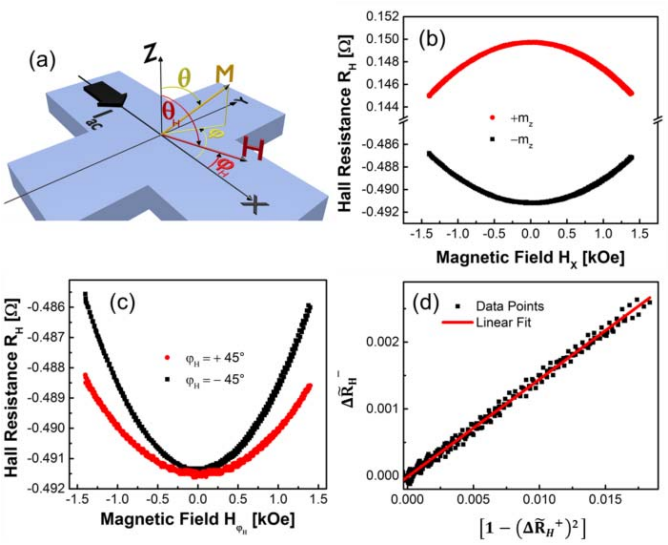

Fig. 1. (a) Schematic of the Hall measurement setup with vector information of the magnetization and the applied magnetic field. (b) Hall resistances as a function of the externally applied field in x-direction. (c) Hall resistance as a function of the applied field with for respective azimuth angle φ_H. (d) $\Delta\tilde{R}_H^-$ as a function of $[1-(\Delta\tilde{R}_H^+)^2]$ with a linear fit.

II. Results

A. PHE to AHE Ratio

The stack structure investigated comprised of Ta(5)/Pt(5)/[Co(0.3)/Ni(0.5)]$_2$/Co(0.3)/IrMn(10)/Ta(2), where the number in brackets correspond to thickness in nm. The film was deposited using DC magnetron sputtering at room temperature. The sample is patterned into a Hall cross structure using electron beam lithography, as shown schematically in Fig. 1(a). The Hall cross structure comprises of 6 μm wide channels

Manuscript received March 10, 2017; revised May 9, 2017; accepted May 9, 2017. Date of publication May 16, 2017; date of current version October 24, 2017. Corresponding author: W. S. Lew (e-mail: wensiang@ntu.edu.sg).

Color versions of one or more of the figures in this paper are available online at http://ieeexplore.ieee.org.

Digital Object Identifier 10.1109/TMAG.2017.2704520

for current as well as for Hall bar. The length of the current channel and Hall bars are 40 μm. Magneto-optical Kerr measurement of the film stack reveals a clear PMA with a coercivity field of 290 Oe and an out-of-plane exchange bias field of 300 Oe.

The magnetization of the sample can be expressed in terms of the spherical coordinate with three degrees of freedom; polar angle θ, azimuth angle φ, and the magnitude of the magnetization vector as saturation magnetization M_S, as shown in Fig. 1(a). The externally applied field $\vec{H}$ can be similarly expressed using spherical coordinate with polar angle θ_H, azimuth angle φ_H, and magnitude H. Here, we investigate SOT and magnetic anisotropy effective fields as a function of applied in-plane magnetic fields. As a result, the polar angle θ_H of the applied field is fixed at 90°. For a sample with PMA, the magnetization orientation aligns along the $\pm z$ orientation and the application of an external in-plane field, leads to a tilting of both the polar (θ) and azimuth (φ) angle of the out-of-plane magnetization.

The magnetization vector in the azimuth orientation follows the externally applied magnetic field, $\varphi = \varphi_H$. The polar orientation of the magnetization vector depends on the interplay between the effective out-of-plane anisotropy field H_K and the externally applied field. For $H \ll H_K$, the polar angle deviation of the magnetization can be written as [8]

$$\theta \approx \frac{H}{H_K}. \tag{1}$$

The contribution of the demagnetizing field on the polar angle of the magnetization is negligible in samples with large H_K. To quantify the SOT effective fields, ac current is applied along the wire axis, x-direction and the Hall voltage is measured across the contacts in the y-direction. An important parameter in estimating the SOT fields using the harmonic measurement technique, is the resistance ratio of PHE (ΔR_P) to AHE (ΔR_A), $\xi = \Delta R_P / \Delta R_A$, which acts as a correcting factor in the experimentally measured SOT fields [9], [10]. ξ can be quantified from the measurement of the first harmonic Hall resistance R_H [11]

$$R_H = \frac{1}{2}\Delta R_A \cos\theta + \frac{1}{2}\Delta R_P \sin^2\theta \sin 2\varphi. \tag{2}$$

From (2), it can be noted that ΔR_A is independent of the azimuth angle of the magnetization vector while the term ΔR_P vanishes for 0° azimuth angle. Fig. 1(b) shows the Hall resistance measured as a function of the external field applied along the x-axis ($\varphi_H = 0°$). At $H = 0$, for sample with $+z$ magnetization orientation, a maximum R_H is obtained, whereas for magnetization along the $-z$ orientation, a minimum R_H is obtained. The magnitude of R_H at $H = 0$, is directly correlated with the anomalous Hall resistance ΔR_A as inherently $\theta = 0°$. Interestingly, we note that in our sample, the magnitude of R_H is different for magnetization aligned along $+z$ and $-z$ orientation. This can be related to the out-of-plane exchange bias effect induced by the antiferromagnetic IrMn layer. The effective ΔR_A is then obtained by averaging the R_H magnitude for the two magnetization orientations at $H = 0$. For our sample, ΔR_A is computed to be 0.641 Ω.

The contribution of PHE to R_H is most significant when the azimuth angle is $\pm 45°$. Though techniques have been devised for determining the PHE resistances using large external fields [12], in this paper, we have adopted an alternative approach. A method using low external field ($H \ll H_K$) is used. From (2), the maximum and minimum values for R_H would occur when the azimuth angle is set to $+45°$ and $-45°$, respectively.

R_H at respective angles φ_H of $\pm 45°$ can be normalized by dividing with the ΔR_A. The normalized R_H at an azimuth angle $\tilde{R}_H^{\varphi_H}$ is then given by $\tilde{R}_H^{\varphi_H} = R_H^{\varphi_H} / \Delta R_A$. Summing $\tilde{R}_H^{\varphi_H}$ measured at azimuth angles of $+45°$ and $-45°$, the following expression can be derived:

$$\Delta \tilde{R}_H^{+} = \tilde{R}_H^{45} + \tilde{R}_H^{-45} = \cos\theta. \tag{3}$$

Similarly, the difference of $\tilde{R}_H^{\varphi_H}$ at angles $\varphi_H = \pm 45°$ can be expressed as

$$\Delta \tilde{R}_H^{-} = \tilde{R}_H^{45} - \tilde{R}_H^{-45} = \xi \sin^2\theta = \xi\left[1 - \left(\Delta \tilde{R}_H^{+}\right)^2\right]. \tag{4}$$

In Fig. 1(c) are the Hall resistance curves as the external field is swept at azimuth angles of $\pm 45°$ and the magnetization of the sample is set along $-z$ orientation. The deviation between the two curves increases as a function of the external field, as at larger fields, the magnetization vector will follow the external field. From (4), the difference between the two curves in Fig. 1(c), $\Delta \tilde{R}_H^{-}$, is calculated and plotted as a function of $[1 - (\Delta \tilde{R}_H^{+})^2]$, as shown in Fig. 1(d). A linear relation is observed and the gradient of the slope gives the term ξ. For our sample structure, the ratio is calculated to be $\xi = 0.146 \pm 0.001$.

B. Perpendicular Magnetic Anisotropy Effective Field

To confirm the calculated, ξ determined using our approach is accurate, we investigated the angular dependence of the perpendicular anisotropy field. As the anisotropy field is a material parameter, it should not vary as a function of the angle of the applied field. From the well-established ac harmonic Hall measurement method, used to characterizing the SOT effective fields, the magnetic anisotropy field H_K can also be obtained.

In PMA structures, the first harmonic Hall voltage signal, in the presence of an in-plane field, is ascribed to the magnetization vector tilting in-plane, changing the polar angle of the magnetization θ

$$V_\omega = \frac{1}{2}[\Delta R_A \cos\theta + \Delta R_P \sin^2\theta \sin 2\varphi] I_{\text{ac}}. \tag{5}$$

By combining (1) and (5) and simplifying using first order Taylor expansion, the tilt in magnetization θ can be used to find H_K. For a sample magnetized along $-z$ orientation, the anisotropy field can be written as

$$\begin{aligned} H_K &= \sqrt{-\frac{1}{2b_\omega}(\Delta R_A - 2\Delta R_P \sin 2\varphi_H) I_{\text{ac}}} \\ &= \sqrt{-\frac{\Delta R_A}{2b_\omega}(1 - 2\xi \sin 2\varphi_H) I_{\text{ac}}} \end{aligned} \tag{6}$$

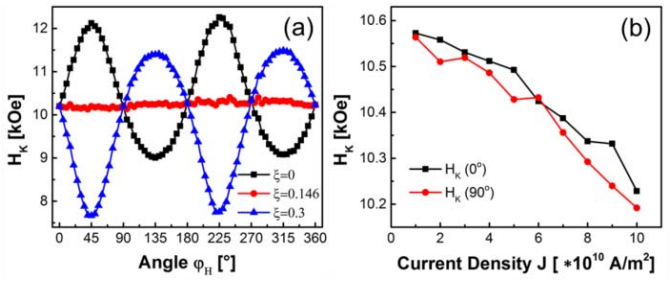

Fig. 2. (a) H_K as a function of the azimuth angle for various ratios ξ at a current density of 1×10^{11} A/m^2. (b) H_K as a function of the current density for azimuth angles of 0° and 90°.

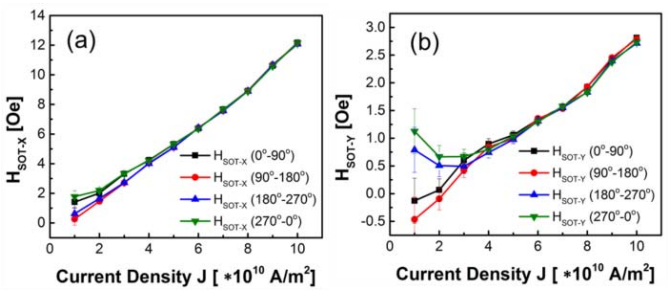

Fig. 3. (a) Damping-like SOT effective fields as a function of the current density for various azimuth angles configurations. (b) Field-like SOT effective fields as a function of the current density for various azimuth angles configurations.

where b_ω is the second derivative of the first harmonic Hall voltage, $b_\omega = \partial^2 V_\omega / \partial H^2$. In Fig. 2(a), the variation of H_K as a function of the azimuth angle is plotted for various ξ. A sinusoidal trend is observed for the representative ξ. However, H_K should not show any angular field dependence as it is an intrinsic material property. For the measured value of $\xi = 0.146$, irrespective of the angle of applied field, a constant H_K is obtained, which is expected. This confirms that our method of calculating the ξ term is accurate. From Fig. 2(a), for all the ξ considered, when the term $\sin 2\varphi_H$ in (5) is zero, the magnitude of H_K can be calculated. H_K is calculated to be 10.2 kOe. The effect of current on the effective anisotropy field is further investigated. Fig. 2(b) shows H_K as a function of the magnitude of the applied ac current when the external field azimuth angles are set at 0° and 90°. As expected, irrespective of the azimuth angle, the effective anisotropy field decreases as the current is increased. A decrease in the effective anisotropy field by ~350 Oe which correspond to a ~3.5% is observed as the current density is increased from 1×10^{10} to 10×10^{10} A/m^2. This reduction in the effective anisotropy is attributed to the SOT-induced effective fields in the sample. The small deviation in the measured magnetic anisotropy fields at the different azimuth angle arises from sample-tilting in our measurement setup which may lead to a small out-of-plane field contribution.

C. SOT Effective Fields

To quantify the SOT effective fields in our structure, first and second harmonic Hall voltages are measured for orthogonal azimuth angles. The second harmonic Hall voltage has been shown to originate from the combination of magnetization change and current-induced effective fields. These current-induced fields are ascribed to SOT effective fields which are aligned in-plane toward the current direction (x-axis) and transverse to the current direction (y-axis).

By taking the ratio of the derivatives of the harmonic voltages, $B_{X,Y} = (\partial V_{2\omega}/\partial H_{X,Y})/(\partial^2 V_\omega / \partial H_{X,Y}^2)$, at respective applied field directions collinear to x- and y-axis, the SOT effective fields can be computed as [9]

$$H_{\text{SOT-}X} = -2\frac{(B_X - 2\xi B_Y)}{1 - 4\xi^2} \tag{7}$$

$$H_{\text{SOT-}Y} = -2\frac{(B_Y - 2\xi B_X)}{1 - 4\xi^2}. \tag{8}$$

As seen from (7) and (8), to account for the ξ factor correction, the characterization of the damping-like or field-like term would require measuring the harmonic voltages for fields applied along both the x- and y-axis. For fields applied along $-x$ or $-y$-axis, the sign of the respective voltage ratio $B_{X,Y}$ has to be corrected according to AHE and PHE symmetries described in (2). In Fig. 3(a) is the corresponding damping-like field ($H_{\text{SOT-}X}$) measured at different orthogonal azimuth angle configurations. $H_{\text{SOT-}X}$ increases linearly as a function of increasing current. Irrespective of the measurement angles, the same $H_{\text{SOT-}X}$ is obtained, which is consistent with (7).

Similarly, the measured field-like term ($H_{\text{SOT-}Y}$) is shown in Fig. 3(b). As expected a linear trend as a function of current is observed. At small current densities, the change in $H_{\text{SOT-}Y}$ is due to the low signal to noise ratio for the second harmonic signal. The Oersted field contribution from the nonmagnetic layers sandwiching the FM layer which acts along $H_{\text{SOT-}Y}$, is computed to be ~0.12 Oe per 1×10^{10} A/m^2 [5].

To extract the SOT effective fields as a function of the azimuth angle of the magnetization, the symmetries arising in the AHE and PHE, as shown in (2) have to be considered. By taking into account the symmetries from AHE and PHE, the SOT effective fields can be obtained by measuring the harmonics voltage at azimuth angles of φ_H and $(90° - \varphi_H)$. The effective fields for sample magnetized along $-z$-axis is then given by [13]

$$H_{\text{SOT-}Y} = \frac{\alpha B_{\varphi_H} + \beta B_{90°-\varphi_H}}{\alpha^2 - \beta^2} \tag{9}$$

$$H_{\text{SOT-}X} = \frac{\beta B_{\varphi_H} + \alpha B_{90°-\varphi_H}}{\beta^2 - \alpha^2} \tag{10}$$

where the parameters α, β, and the ratio B_{φ_H} are

$$\alpha = -\frac{1}{2}\sin\varphi_H + \frac{\xi \cos 2\varphi_H}{1 - 2\xi \sin 2\varphi_H}\cos\varphi_H \tag{11}$$

$$\beta = -\frac{1}{2}\cos\varphi_H - \frac{\xi \cos 2\varphi_H}{1 - 2\xi \sin 2\varphi_H}\sin\varphi_H \tag{12}$$

$$B_{\varphi_H} = \alpha H_{\text{SOT-}Y} + \beta H_{\text{SOT-}X}. \tag{13}$$

Similarly, using the symmetry at φ_H and $(270° - \varphi_H)$, the SOT effective fields can be computed as

$$H_{\text{SOT-}Y} = \frac{\alpha B_{\varphi_H} - \beta B_{270°-\varphi_H}}{\alpha^2 - \beta^2} \tag{14}$$

$$H_{\text{SOT-}X} = \frac{\beta B_{\varphi_H} - \alpha B_{270°-\varphi_H}}{\beta^2 - \alpha^2}. \tag{15}$$

The first and harmonic voltages were measured as a function of the azimuth angle in 5° steps. The derivatives of the harmonic

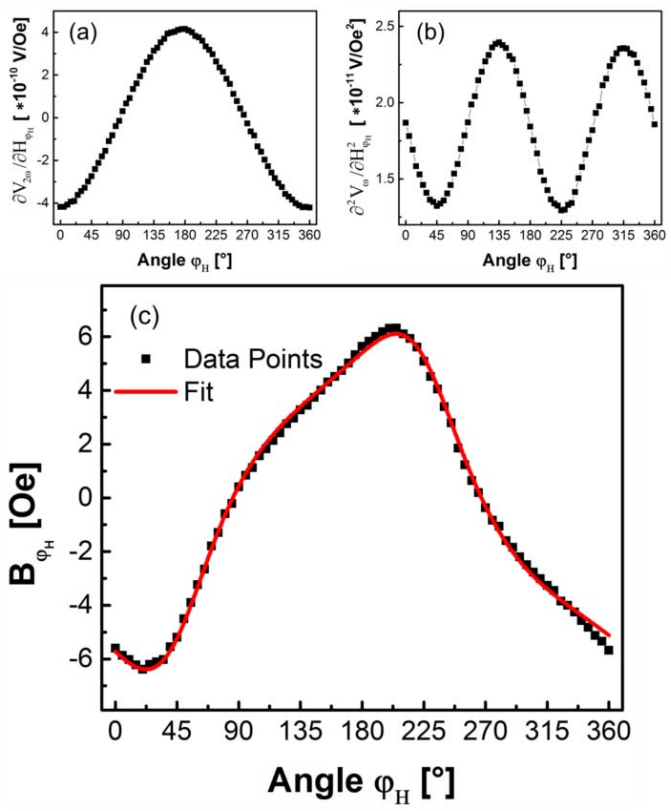

Fig. 4. Current density in the wire was fixed at 1×10^{11} A/m^2. (a) First derivate of second harmonic Hall voltage as a function of the azimuth angle. (b) Parabolic fitting parameter of the first harmonic Hall voltage as a function of the azimuth angle from the applied field. (c) Ratio B_{φ_H} as a function of the azimuth angle φ_H. The red curve is the fitting function from (13).

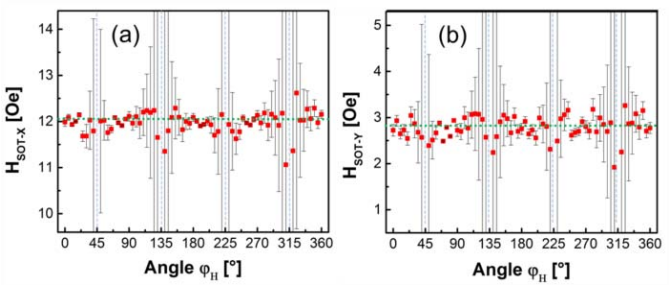

Fig. 5. Averaged SOT effective fields as a function of the azimuth angle at a current density of 1×10^{11} A/m^2 for (a) damping-like field and (b) field-like field. The blue dashed lines indicate the asymptotes where no effective field can be computed and the green dashed lines indicate the mean value.

voltages for each angle are obtained by using the parabolic and linear fitting [8], [9]. In Fig. 4(a) is the first derivative of the second harmonic signal as a function of different azimuth angles. A predominant $-\cos\varphi_H$ relation is clearly seen. The second derivative of the first harmonic signal for different angles is presented in Fig. 4(b). As expected, a $-\sin 2\varphi_H$ relation is obtained which is a result of the PHE signal. The ratio of the second harmonic to first harmonic derivatives, B_{φ_H} is plotted in Fig. 4(c). The angular variation of B_{φ_H} is in good agreement with (13) as shown by the fitting curve in Fig. 4(c). This implies that our theoretical derivation is in good approximation with the experimental measurements.

The extracted $H_{\text{SOT-}X}$, from (10) and (14), and $H_{\text{SOT-}Y}$, (9) and (13) of the SOT effective fields as a function of angle is plotted in Fig. 5. The mean $H_{\text{SOT-}X}$ is 12.1 Oe while the mean $H_{\text{SOT-}Y}$ is 2.8 Oe per 1×10^{11} A/m^2. Both SOT effective fields exhibit small variations from the mean value as a function of the azimuth angle. For the $H_{\text{SOT-}Y}$, Fig. 5(b), local minima are observed at azimuth angles of 45°, 135°, 225°, and 315° with symmetry-axes where $\alpha^2 = \beta^2$. Similar trend can be seen in Fig. 5(a) as well. We expect that this trend can be more pronounced in samples with larger SOT effective fields.

III. Conclusion

A method to quantify the PHE to AHE ratio using harmonic Hall voltage scheme at low applied fields has been proposed and experimentally validated. This enables direct quantification of the SOT effective fields as a function of the magnetization azimuth angle with respect to the current direction. Our theoretical equation for obtaining angular variation of the ratio of the derivatives of the harmonic voltages is in good agreement with the measured experimental values.

Acknowledgment

This work was supported in part by the Singapore National Research Foundation under Grant NRF-CRP9-2011-01, in part by the Industry-IHL Partnership Program under Grant NRF2015-IIP001-001, and in part by the MOE-AcRF Tier 2 under Grant MOE 2013-T2-2-017.

References

[1] I. M. Miron *et al.*, "Perpendicular switching of a single ferromagnetic layer induced by in-plane current injection," *Nature*, vol. 476, no. 7359, pp. 189–193, 2011.

[2] L. Liu, O. J. Lee, T. J. Gudmundsen, D. C. Ralph, and R. A. Buhrman, "Current-induced switching of perpendicular magnetized magnetic layers using spin torque from the spin Hall effect," *Phys. Rev. Lett.*, vol. 109, p. 096602, Aug. 2012.

[3] C.-F. Pai, L. Liu, Y. Li, H. W. Tseng, D. C. Ralph, and R. A. Buhrman, "Spin transfer torque devices utilizing the giant spin Hall effect of tungsten," *Appl. Phys. Lett.*, vol. 101, no. 12, p. 122404, 2012.

[4] K. Garello *et al.*, "Symmetry and magnitude of spin–orbit torques in ferromagnetic heterostructures," *Nature Nanotechnol.*, vol. 8, pp. 587–593, Jul. 2013.

[5] S. Fukami, C. Zhang, S. DuttaGupta, A. Kurenkov, and H. Ohno, "Magnetization switching by spin–orbit torque in an antiferromagnet—Ferromagnet bilayer system," *Nature Mater.*, vol. 15, pp. 535–541, Feb. 2016.

[6] Y.-C. Lau, D. Betto, K. Rode, J. M. D. Coey, and P. Stamenov, "Spin–orbit torque switching without an external field using interlayer exchange coupling," *Nature Nanotechnol.*, vol. 11, pp. 758–762, May 2016.

[7] U. H. Pi *et al.*, "Tilting of the spin orientation induced by Rashba effect in ferromagnetic metal layer," *Appl. Phys. Lett.*, vol. 97, p. 162507, Oct. 2010.

[8] J. Kim *et al.*, "Layer thickness dependence of the current-induced effective field vector in Ta/CoFeB/MgO," *Nature Mater.*, vol. 12, pp. 240–245, Mar. 2013.

[9] M. Hayashi, J. Kim, M. Yamanouchi, and H. Ohno, "Quantitative characterization of the spin-orbit torque using harmonic Hall voltage measurements," *Phys. Rev. B, Condens. Matter*, vol. 89, p. 144425, Apr. 2014.

[10] S. Woo, M. Mann, A. J. Tan, L. Caretta, and G. S. D. Beach, "Enhanced spin-orbit torques in Pt/Co/Ta heterostructures," *Appl. Phys. Lett.*, vol. 105, p. 212404, Nov. 2014.

[11] K. Okamoto, "A new method for analysis of magnetic anisotropy in films using the spontaneous Hall effect," *J. Magn. Magn. Mater.*, vol. 35, nos. 1–3, pp. 353–355, 1983.

[12] X. Qiu *et al.*, "Angular and temperature dependence of current induced spin-orbit effective fields in Ta/CoFeb/MgO nanowires," *Sci. Rep.*, vol. 4, p. 04491, Apr. 2014.

[13] C. Engel, S. Goolaup, F. Luo, and W. S. Lew, "Quantitative characterization of Pt/Co/Pt/Co/Ta heterostructure magnetization azimuth angle dependence on spin-orbit torque effective fields," 2017, [Online]. Availble: https://arxiv.org/abs/1706.01622